DOI 10.5162/Ultrasonic2025/A4-a2

Ultrasonic Guided Waves for Gas Bubble Removal on Optical Sensor Surfaces

Oliver Blaschke[1], Dennis Bernhardt-Famulla[2], Stephanie Holz[2], and Klaus Stefan Drese[1]
[1]Coburg University of Applied Sciences and Arts, Institute for Sensor and Actuator Technology, Coburg, Germany
[2]Dr. Küke GmbH, Wedemark, Germany
oliver.blaschke@hs-coburg.de

Abstract: This study demonstrates a method for gas bubble removal from glass surfaces using acoustic standing wave fields. Piezoelectric transducers generate targeted frequencies, creating radiation forces that move bubbles toward antinodes. By incorporating bubble resonance frequencies, detachment efficiency is enhanced. Simulations and experiments confirmed effective wave formation and bubble migration. A burst-mode excitation minimized thermal load, providing a non-invasive solution for maintaining optical sensor performance in liquid environments.

Keywords: bubbles, ultrasonic bubble manipulation, ultrasonic transducers, acoustics, standing waves

Introduction

The presence of gas bubbles adhering to glass surfaces in water poses a critical issue for optical sensors utilized in the context of water quality measurements. These bubbles induce distortions in light paths through the process of refraction, thereby leading to inaccuracies in parameter estimation. The presence of even small bubbles has the capacity to significantly alter sensor readings by introducing optical artifacts that interfere with the transmission and detection of light. Therefore, the objective of this study is to explore the use of ultrasonic guided acoustic waves as a means to effectively remove bubbles from glass surfaces. This technique utilizes the interaction of ultrasonic acoustic waves with the water-glass interface, forming standing wave fields, thereby inducing radiation forces that influence bubble motion. A further point of this study is whether the excitation of the bubbles at their resonance frequency at the same time can improve the manipulation of the bubbles due to reduced bonding to the adhering surface.

Method

Acoustic waves that propagate along the solid-water interface at specific frequencies and wavelengths generate an acoustic standing wave field in the adjacent fluid. Fluctuations in pressure within the acoustic field create stationary nodes and fluctuating antinodes. The wavelength necessary for a standing wave field to form depends on the width of the system. This results in a set of wavelengths that are integer divisors of twice the width of the system:

$$\lambda = \frac{2L}{n};\ n = 1, 2, 3, ... \tag{1}$$

The acoustic radiation force in the standing wave field causes the gas bubbles to move toward the antinode positions within the fluid region. This leads to increased movement and eventually causes the bubbles to move away from the glass surface [1].

The radiation force is defined with the time-averaged first-order pressure $\langle p \rangle$ and velocity $\langle v \rangle$ as [2], [3]:

$$F_{rad} = \int_{\partial\Omega} \left\{ \left[\frac{1}{2}\kappa_0 \langle p^2 \rangle - \frac{1}{2}\rho_0 \langle v^2 \rangle \right] n + \rho_0 \langle (n \cdot v) v \rangle \right\} \tag{2}$$

With κ_0 as the compressibility of the bulk fluid as $\kappa_0 = 1/(\rho_0 c_0^2)$ where ρ_0 and c_0 are the density and velocity of sound of the fluid, respectively.

While the acoustic field is active, the bubbles are trapped within the antinodes. When the field is shut off, buoyancy effects transport the bubbles away. To increase the effect, the resonance characteristic of the gas bubbles themselves was used. Depending on their size, bubbles have resonance frequencies at which they oscillate. This oscillating movement reduces the bubbles' adherence to the glass surface, allowing them to be more efficiently removed by the acoustic radiation force of the standing wave field. For constrained gas bubbles, for which the influence of surface tension is not negligible, the resonance frequency can be derived from the Rayleigh-Plesset equation, as described in [4]:

DOI 10.5162/Ultrasonic2025/A4-a2

$$R\ddot{R} + \frac{3\dot{R}^2}{2} = \frac{1}{\rho}\left\{\left(p_0 + \frac{2\sigma}{R_0} - p_v\right)\left(\frac{R_0}{R}\right)^{3\gamma} + p_v - \frac{2\sigma}{R} - \frac{4\eta\dot{R}}{R} - p_0 - P(t)\right\} \tag{3}$$

Here, the oscillating bubble radius R in an acoustic field depends on its first- and second-order time derivatives $\dot{R}$ and $\ddot{R}$ as well as the surface tension acting on the bubble σ, the fluid density ρ_0 and the viscosity η, as well as the hydrostatic pressure p_0 and the vapor pressure inside the bubble p_v and the initial bubble radius R_0. $P(t)$ is the time-dependent pressure variation from the acoustic field and γ is the polytropic index.

For the assumption of small amplitude variations in bubble radius, the resonance frequency ω_0 can be calculated with [4]:

$$\omega_0 = \frac{1}{R_0\sqrt{\rho}} \sqrt{\left\{3\gamma\left(p_0 + \frac{2\sigma}{R_0} - p_v\right) - \frac{2\sigma}{R_0} + p_v - \frac{4\eta^2}{\rho R_0^2}\right\}} \tag{4}$$

The material properties as can be seen in table 1. According to Figure 1 the resonance frequency for bubbles of the size in the range between 100 µm and 2 mm ranges from 0.5 kHz to 13 kHz.

Tab. 1: Material properties of gas bubbles and water at 20°C.

$\rho/\frac{\mathrm{kg}}{\mathrm{m}^3}$	998
$\sigma/\frac{\mathrm{N}}{\mathrm{m}}$	0.0728
$\eta/\mathrm{Pa}\cdot\mathrm{s}$	1.001×10^{-3}
p_0/Pa	101 325
p_v/Pa	2340
γ	1.4

For the experimental setup, a measurement chamber with dummy sensors as optical sensors was constructed in order to serve as a basis for gas bubble removal. The housing is depicted in Figure 2. For the generation of ultrasonic frequencies, piezoelectric transducers were considered because they can act on a wide range of frequencies and can be driven at high voltages for large deflections. Since the space for attaching the transducers was limited, they were placed directly on the top side of the quartz glass

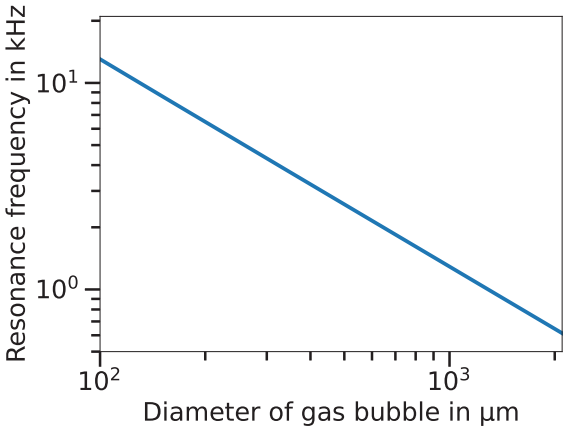

Fig. 1: Resonance frequency of gas bubbles in water for different bubble diameters.

surface, next to the optical sensor dummy. Lead zirconate titanate (PZT) transducers (PIC 255 material, PI Ceramic GmbH, Lederhose, Germany), measuring 25 mm $\times$ 2 mm $\times$ 1 mm were used. Two transducers were placed in a row on both sides of the dummy to span its entire length, reaching a total length of 50 mm. The goal was to remove any gas bubbles from the glass surface under the dummy elements. The same procedure was carried out on the back of the housing because there is another dummy element there. The prepared measurement chamber is depicted in Figure 2.

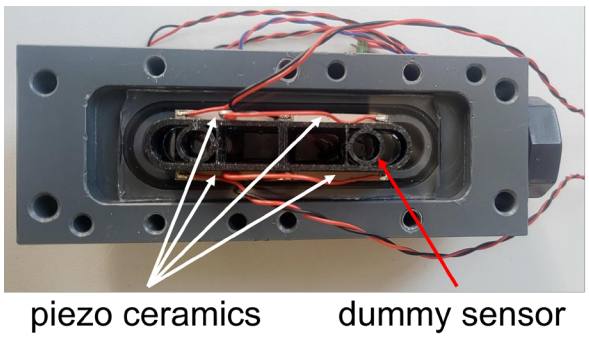

Fig. 2: Measurement chamber with dummy sensor and prepared glass surface with piezo transducers.

The necessary wavelengths for the standing wave fields were found using equation (1) where the system's width, L, was 12 mm. This resulted in a set of wavelengths and with the speed of sound in water being 1480 m/s, distinct frequencies were determined. FEM simulations were conducted in COMSOL Multiphysics software to prove the excitation concept on

DOI 10.5162/Ultrasonic2025/A4-a2

the geometry of the measurement chamber in beforehand. The three-dimensional simulations included the chamber's fluid volume as well as the 3 mm thick quartz glass plates. The excitation of the standing wave fields with the related driving frequencies was modeled on top of the glass plates to emulate the actuation with the piezo ceramics in the experimental stage. To demonstrate standing wave excitation in a fluid volume, a special measurement chamber was constructed. The side walls were cut out and replaced with glass plates, one of which was coated with a primer. The experimental setup involved continuously exciting the standing wave field at a frequency of 370 kHz and measuring the pressure field inside the fluid with a laser Doppler vibrometer (PSV-400M, Polytec GmbH, Waldbronn, Germany). The results were then compared with those of the associated finite element method (FEM) simulation. Figure 3 compares the standing wave fields from the experiment and the simulation, showing that the results agree qualitatively. This indicates that the generation of the standing wave field and the corresponding radiation force, which moves the gas bubbles toward the fluid volume and away from the glass surface, operated as intended. The final step was to optimize the actuation to remove the bubbles faster and more efficiently.

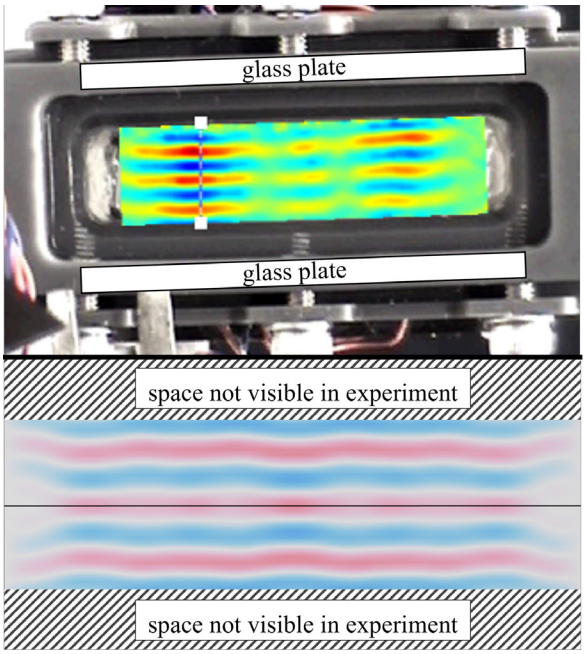

Fig. 3: Laser Doppler vibrometer measurement of pressure field inside measurement chamber (top). FEM simulation of same excitation at 370 kHz (bottom).

The final driving signal for the transducers was designed to fulfill two tasks. First, a standing wave field had to be generated. Second, the resonance frequency of the different bubble sizes had to be met. To this end, a chirp signal was designed to encompass the frequency range between 0.5 kHz and 7 kHz, striking a balance between the findings of Figure 1 and the overall signal length and, consequently, the thermal load on the piezo ceramics. The chirp signal was alternated with continuous high-frequency sinusoidal signals at the following frequencies: 308.33 kHz, 370.00 kHz, 431.67 kHz and 493.33 kHz. For clarification, the excitation signal and the resulting frequency spectrum are depicted in Figure 4. The signal was driven in burst mode, and the burst delay was chosen to be 112 ms to ensure that the piezo ceramics would not overheat, even with long-term usage. In the experimental setup the signal was generated with a function generator (33521A, Agilent Technologies, Waldbronn, Germany) and amplified to 288 Vpp with a voltage amplifier (A 1230-02, Dr. Hubert GmbH, Bochum, Germany) before being fed into the piezo ceramics.

Results

The experimental investigation of gas bubble removal revealed that combining the resonance frequency and the standing wave approach significantly optimizes bubble migration, enabling efficient removal across the relevant sensor surface. Figure 5 shows the initial gas-bubble-contaminated surface, as well as the stages of the cleaned surface after up to three burst cycles of the excitation signal shown in Figure 4. Most of the adhering gas bubbles detached during the first burst cycle, which occurred after 40 µs. The last few bubbles detached after the third cycle, which occurred after about 340 µs. The final image on the right in Figure 5 shows the bubble-free surface after the bubbles in the fluid were driven away by buoyancy.

For cases involving excitation at only the resonance frequencies of the gas bubbles or the excitation of only the standing wave field, the bubble removal results were much lower than those in the combined, alternating case presented in the Methods section. The frequencies for the standing wave field were chosen based on their effectiveness. Frequencies lower than 300 kHz did not significantly affect the bubbles. Frequencies higher than 500 kHz were also not suitable for this task because increased overall power consumption resulted in a lower maximum voltage to prevent thermal destruction of the piezo ceramics. In this case, frequencies higher than 500 kHz did not offer an increase in bubble manipulation.

DOI 10.5162/Ultrasonic2025/A4-a2

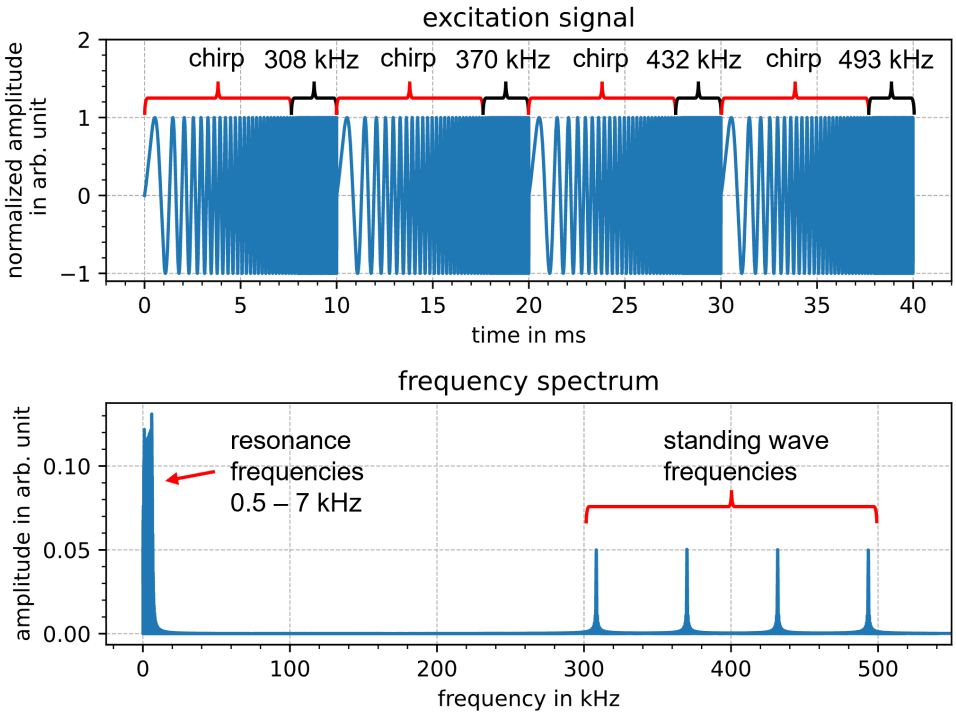

Fig. 4: One period of the excitation signal (top). Corresponding multi-band frequency spectrum (bottom).

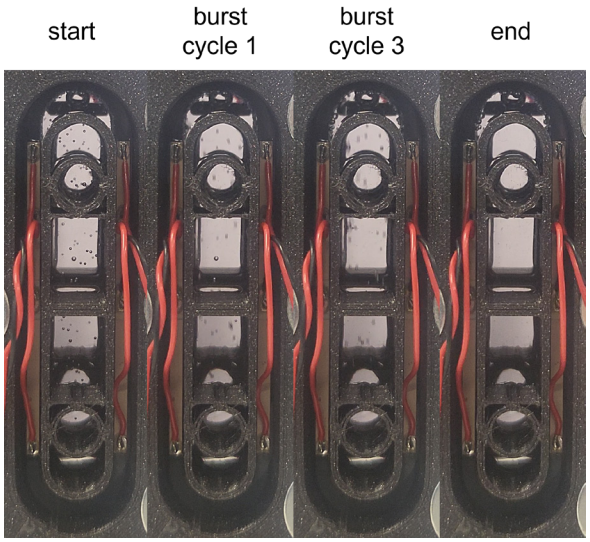

Fig. 5: Applied strategy for bubble removal. Left to right: start with no actuation, few bubbles on surface after the first burst cycle, no bubbles on surface after three burst cycles, result after shutting off.

Conclusion

The brief cleansing period and low power usage of burst mode actuation offer an energy-efficient, non-invasive method that maintains long-term precision and reliability of optical sensors in liquid environments. Unlike mechanical or chemical cleaning, this approach avoids sensor degradation or contamination. Additionally, ultrasonic wave parameters can be adjusted in real time to adapt to changes in temperature and flow conditions. This makes acoustic bubble removal a scalable solution for water quality monitoring and advances acoustic bubble migration technology, enhancing optical sensor performance.

Acknowledgment

This research was funded by the German Federal Ministry of Research, Technology and Space (BMFTR) within the program "KMU-innovativ" under grant number 02WQ1677B.

References

[1] X. Xi, F. B. Cegla, M. Lowe *et al.*, 'Study on the bubble transport mechanism in an acoustic standing wave field,' *Ultrasonics*, vol. 51, no. 8, 2011.

[2] H. Bruus, 'Acoustofluidics 7: The acoustic radiation force on small particles,' *Lab on a Chip*, vol. 12, no. 6, 2012.

[3] W. Lauterborn and T. Kurz, 'Physics of bubble oscillations,' *Reports on Progress in Physics*, vol. 73, no. 10, 2010.

[4] T. G. Leighton, *The acoustic bubble*. London San Diego New York [etc.]: Academic press, 1994.